crystals

MDPI

Article

Influence of Chemical Composition and Electro-Steel Sheets Manufacturing Parameters on the Adhesion of an Electro-Insulating Self-Bonding Varnish Layer

Vanda Tomková [1], Miroslav Tomáš [2,*], Stanislav Németh [1], Matúš Horváth [3], Vladimír Kundracík [1], Emil Evin [2], Ján Slota [2], Anna Guzanová [2] and Iveta Filipovská [4]

[1] USSE Research and Development, U.S. Steel Košice s.r.o., Vstupný Areál U.S. Steel, 044 54 Kosice, Slovakia; vandatomkova@sk.uss.com (V.T.); snemeth@sk.uss.com (S.N.); vkundracik@sk.uss.com (V.K.)
[2] Institute of Technology and Materials Engineering, Faculty of Mechanical Engineering, Technical University of Kosice, Mäsiarska 74, 040 01 Kosice, Slovakia; emil.evin@tuke.sk (E.E.); jan.slota@tuke.sk (J.S.); anna.guzanova@tuke.sk (A.G.)
[3] Magna Powertrain s.r.o., Perínska Cesta 282, 044 58 Kechnec, Slovakia; matus.horvath@magna.com
[4] USSK Test Laboratories, U.S. Steel Košice s.r.o., Vstupný Areál U.S. Steel, 044 54 Kosice, Slovakia; ifilipovska@sk.uss.com
* Correspondence: miroslav.tomas@tuke.sk; Tel.: +421-55-602-3524

Abstract

One promising innovative joining process for non-oriented electrical sheets is based on an electro-insulating layer combined with a self-bonding varnish. The aim of this study was to investigate the adhesion of the self-bonding varnish as evaluated by a lap-shear test. During the experiments, non-oriented electrical steels with low to high silicon content were analyzed and tested. The Si content, the bond thickness, and the surface roughness Ra, as well as the selected steel production parameters—such as the radiation tube furnace temperature (RTF), the grain growth temperature (i.e., heating temperature (HF)), the peak metal temperature (PMT), and the annealing atmosphere (dry or humid, controlled by dew point)—were considered as the variables. The results showed that the lap-shear strength was independent of the surface roughness within the investigated range. In contrast, the bond thickness exhibited a weak positive effect on the lap-shear strength, while the Si content showed condition-dependent behavior. The RTF and the HF resulted in a relatively stable mechanical performance, whereas the PMT and the humid annealing atmosphere were identified as critical factors influencing adhesion.

Keywords: non-oriented electrical steel; self-bonding varnish; tensile lap-shear test; lap-shear strength; adhesion of the varnish

Check for updates

Academic Editors: Shilong Liu, Yishuang Yu, Qizhe Ye and Yangxin Wang

Received: 6 March 2026
Revised: 8 April 2026
Accepted: 8 April 2026
Published: 10 April 2026

1. Introduction

Currently, the growing interest in ecological and sustainable mobility is driving an increased production of electric vehicles. The core, made of magnetically soft materials, is a fundamental and integral part of electric motors, along with the windings and insulation systems [1]. The most critical part of such an electric drive is the stator. It consists of numerous thin, laminated steel sheets, so-called laminations, stacked on top of each other. These soft magnetic cores are continuously magnetized and demagnetized to conduct and amplify the magnetic flux. To reduce iron losses during operation, both stator and rotor cores are usually made of thin, layered iron–silicon sheets that are electrically insulated from each other [2,3].

The production quality of such a laminated stator core is influenced by fundamental process steps such as the cutting, joining, and winding of non-oriented electrical steel. Potential sources of losses can arise during each of these phases [4]. At high frequencies, the eddy current losses dominate over the hysteresis losses, thereby contributing to the majority of the total losses. Various manufacturing technologies for joining laminations are often described and compared in the literature to highlight differences and emphasize their respective advantages [5]. With the increasing demands for electric motors in the automotive sector, both the material selection and the corresponding manufacturing processes are continuously being optimized.

One of the promising innovative joining processes is based on an electro-insulating layer combined with the so-called self-bonding varnish. This approach provides one of the most effective connections of rotor and stator laminations in magnetic circuits. In addition to its main function of creating an insulating layer between the laminations, the electro-insulating varnish protects the metal surfaces from corrosion and affects the magnetic properties of steel [6,7]. In general, it combines the properties of varnish and glue: under the combined influence of heat and pressure, the composition of the varnish changes, forming a solid bond between the materials. The steel sheets coated with a self-bonding varnish layer are widely used in the production of electric motor cores, where individual stator and rotor laminations are bonded together. Full-surface bonding with self-bonding varnish, compared to conventional joining techniques such as bonding, welding, or clamping, offers multiple advantages, including design flexibility, mechanical stability, and preservation of magnetic properties [8,9].

Self-bonding varnish enables a versatile design by eliminating the need to consider manufacturing constraints such as joint or weld locations, thereby allowing for a more efficient electric motor. Compared to bonding and welding, this method is the gentlest joining technique, as it does not alter the microstructure through mechanical deformation (as in bonding) or thermal processing (as in welding). Consequently, the magnetic properties are not significantly affected. Face-bonding provides tight dimensional tolerances and excellent dimensional stability, as the individual laminations are joined at discrete points and face-bonded joints are commonly employed between these laminations [9].

Compared to bonding and welding, self-bonding varnish bonding does not cause any short circuits between the individual laminations. This results primarily in a reduction in eddy current losses, leading to an increased efficiency of the magnetic circuit and a decrease in the total specific losses. It also increases the shape accuracy and rigidity of the individual stuck. A significant advantage is the reduction in noise during the operation of the stator and rotor bundles at high frequencies (400 to 1200 Hz), as the individual lamellas are firmly bonded, which eliminates unwanted vibrations and sound. Full-surface bonding also improves thermal conductivity in the bundle, as the self-bonding varnish provides better thermal conductivity compared to the air gaps typically formed in bonding or welding processes [10].

Non-oriented electrical steel coated with self-bonding varnish can be cut without additional lubricants during processing. Self-bonding varnish provides a lubricating effect, which ultimately extends the service life of the pressing tools. The laminations are stacked sequentially, and the subsequent application of heat and pressure causes bonding through the softening and hardening of the adjacent varnish layers. The required pressure depends on the flatness of the steel, the surface microgeometry (as characterized by the roughness parameters), and the thickness of the coating [11,12].

Self-bonding varnish is a functional coating for non-oriented electrical steel. In addition to its insulating properties, which prevent eddy current losses between laminations, the quality of the varnish is primarily determined by factors such as adhesion [13]. The leakage

https://doi.org/10.3390/cryst16040253

of the varnish between laminations during the bonding process can be problematic [10,12], while adhesion is critical for the quality and stability of the package [14]. Adhesion is assessed using standardized test methods, such as the floating roller test according to EN 1464 for rapid bonding or the tensile lap-shear test according to EN 1465 [15,16]. A standardized method for assembling the lamination stack is required to ensure reproducible results for each of these test methods.

The tensile lap-shear test employed in this study provides quantitative information on the lap-shear strength of the bonded joints. When the test specimens are subjected to tension, the results reflect the quality of the adhesive bond. Unlike the roller peel test, the measured adhesive strength in the lap-shear test is independent of the steel strip's thickness and mechanical strength.

The article focuses on electro-insulating varnish with self-bonding properties, which, in addition to its main function (creating an insulating layer between the lamination of magnetic circuits), also protects metal surfaces from corrosion and influences the magnetic properties of steel. The aim of the study is to establish the correct production procedure and surface quality: the heat treatment of non-oriented electrical steels in relation to the adhesion of the bonding varnish and to verify the sufficient strength and quality of the connection between these steels, which represent the individual laminations in stator bundles.

2. Materials and Methods

2.1. Experimental Material

2.1.1. Chemical Composition

The experimental study of a self-bonding varnish adhesion to the non-oriented electrical steel was carried out on three grades of steel that differ in Si and Al content (shown in Table 1), while the content of the other elements is mentioned as nominal values. The steel grade (A) was 0.65 mm thick with a low Si content; the steel grade (B) was 0.65 mm thick with a medium Si content; and the steel grade (C) was 0.50 mm thick with a high Si content. All the tested steel grades were coated on both sides with an electro-insulating layer of self-bonding varnish, with a thickness of 2.85 ± 1.25 µm per side.

Table 1. The chemical composition of the tested steel grades [wt.%].

Steel Grade	C	Si	Al	S	N
(A)	<0.006	0.95 ± 0.25	0.13 ± 0.04	<0.01	<0.007
(B)		1.35 ± 0.15	0.26 ± 0.05		
(C)		2.95 ± 0.25	1.02 ± 0.13		

The Si content in the experimental non-oriented electrical steels allows for variation in both the magnetic properties—specifically, the maximum specific loss of 8 W/kg for grade (A), 4.7 W/kg for grade (B), and 2.7 W/kg for grade (C)—and the electrical resistance of steels (25 $\mu\Omega/cm^2$ for grade (A), 35 $\mu\Omega/cm^2$ for grade (B), and 50 $\mu\Omega/cm^2$ for grade (C). Nevertheless, silicon has detrimental effects, as its tendency to induce embrittlement restricts the production of non-oriented electrical steels with silicon contents above approximately 3 wt.% [17–19].

2.1.2. Production Parameters

The final processing of the experimental non-oriented electrical steels was carried out on a continuous annealing line. The annealing took place at different temperatures and consisted of a few heating sections and two holding sections of the furnace. In the first section of the furnace either a humid or dry atmosphere was applied. The humid atmosphere (dew point above +30 °C), in which the humidity is maintained by the water vapor content in the furnace, allowed for the control of the steel's carbon content and prevented aging, which can significantly deteriorate the magnetic properties. The dry atmosphere (dew point below −15 °C) was applied for the steels with a low carbon content. In the second furnace section, a higher temperature was typically applied to promote optimal grain growth for the desired magnetic properties. In this section, the dew point (DP) remained below −55 °C [20–24].

During the production of the non-oriented electrical steel grades, boundary conditions were verified to ensure the achievement of an optimal microstructure and balanced electrical and magnetic properties in accordance with the company standards. The production process itself was optimized by the variability of:

- RTF—radiation tube furnace temperature.
- HF—heating furnace (grain growth temperature, i.e., recrystallization temperature).
- PMT—peak metal temperature.

The non-oriented electrical steels were produced under both dry and humid atmospheres, with the individual parameters varied within the ranges indicated in Tables 2 and 3, respectively.

Table 2. The intervals of selected processing parameters when produced in a dry atmosphere.

Steel Grade	RTF [°C]	HF [°C]	PMT [°C]
(A)		Not produced	
(B)	660–890	1020–1100	165–185
(C)	740–860	1070–1090	160–170

Table 3. The intervals of selected processing parameters when produced in a humid atmosphere.

Steel Grade	RTF [°C]	HF [°C]	PMT [°C]
(A)	870–940	880–900	150–175
(B)	845–855	1090–1110	170–200
(C)	735–920	1080–1120	165–220

2.1.3. Self-Bonding Varnish Thickness

The steel grades used in the experiments are intended for the stator and rotor laminations, which are bonded together by applying a special self-bonding varnish and curing it. The interlaminar layer must fulfill two basic functions: adhesion and electrical insulation. The self-bonding varnish used in the experiments was a purely organic coating containing specific bonding agents based on epoxy resins and is free of chromium. It is water-dilutable and can be easily removed using acetone-based solvents. These agents are specially designed to improve the electrical and mechanical properties of the lamination, ensuring optimal performance. Consequently, the self-bonding varnish provides a precise and uniform connection, significantly reducing energy losses and improving the overall efficiency of the electrical components.

The thickness of the insulating layer (Figure 1) on the non-oriented electrical steels was measured using a thickness gauge, Fischerscope MMS PC2—Betascope module (Helmut Fischer Group, Sindelfingen, Germany), which determined the thickness based on the interaction between the ionizing radiation and the insulating layer. When the beta particles hit the material, a portion of them was backscattered, with the scattering behavior depending on the atomic number of the material. The radioisotope C-14 was used as the radiation source. The radiological principle is suitable for all types of film and substrate combinations, provided that the difference between the atomic numbers of the coating material and the substrate is at least 5.

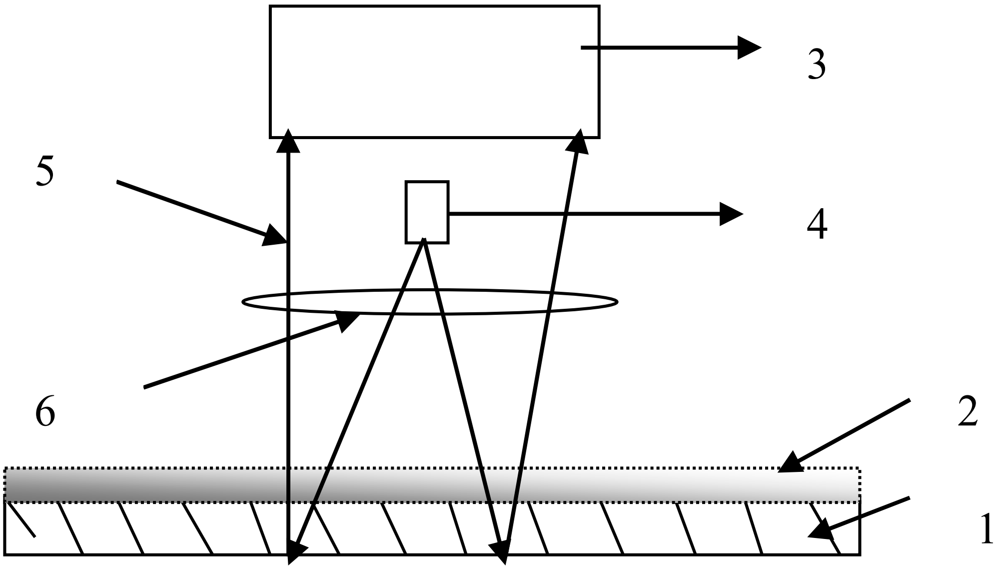

Figure 1. The insulation layer thickness measurement principle: 1—substrate, 2—layer, 3—counter, 4—radioisotope, 5—backscattered beta particles, 6—slot.

2.1.4. Surface Microgeometry

The surface microgeometry parameters were measured using a calibrated device, Hommel Tester T2000 (Hommelwerke, Schwenningen, Germany). The measurement conditions are summarized in Table 4. The parameters evaluated included the Ra (arithmetic mean of profile deviation), the Rz (maximum profile height) according to ISO 21 920-2 [25], and the RPc (number of peaks). The measurements were performed on all sheet metal samples from both sides (Top and Bottom) at five evenly spaced points on each sample.

Table 4. The surface microgeometry measuring conditions.

Measuring Device	Hommel tester T2000
Stylus tip	TKPK100 (two sliding surfaces)
Stylus tip: cone angle	Ø 5 µm ($\alpha = 90°$)
Total measurement length	Lt = 15.0 mm
Evaluated measurement length	Ln = 12.5 mm
Basic measurement length Cut-off	Lr = 2.5 mm
Section lines C1, C2	±0.5 µ
Filter	M1

2.2. Tensile Lap-Shear Test

The processing of these varnishes was carried out in two stages. In the first stage, the varnish was applied in liquid form to the non-oriented electrical steel using rollers on the coating line, followed by curing in an oven at 220–240 °C for 30 s or 200–230 °C for 60 s. Subsequently, in the second stage, the individual pairs of sheets were glued/joined using the varnish in its dried state under pressure, with a curing temperature of 210 °C. A solid joint was achieved, assuming that the varnish had fully reacted after the sheets were bonded. These varnishes are resistant to permanent exposure to temperatures up to 270 °C.

The tensile lap-shear test was performed in accordance with EN 1465 [16], and the maximum lap-shear strength was measured at a crossbar constant speed of 10 mm.min^{-1}. The commonly required minimum lap-shear strength is 10 MPa. The principle of test preparation is shown in Figure 2. The samples were prepared to a size of 62 mm × 25 mm, with a tolerance of ±0.25 mm in width and +0.1 mm in length. Consequently, the length of the glued joint was within the range of 12.25 to 12.75 mm as required by the standard (Figure 2d). Then, 10 samples were taken from each coil, and these were marked on the top surface to ensure the correct positioning of surfaces during gluing (top to bottom).

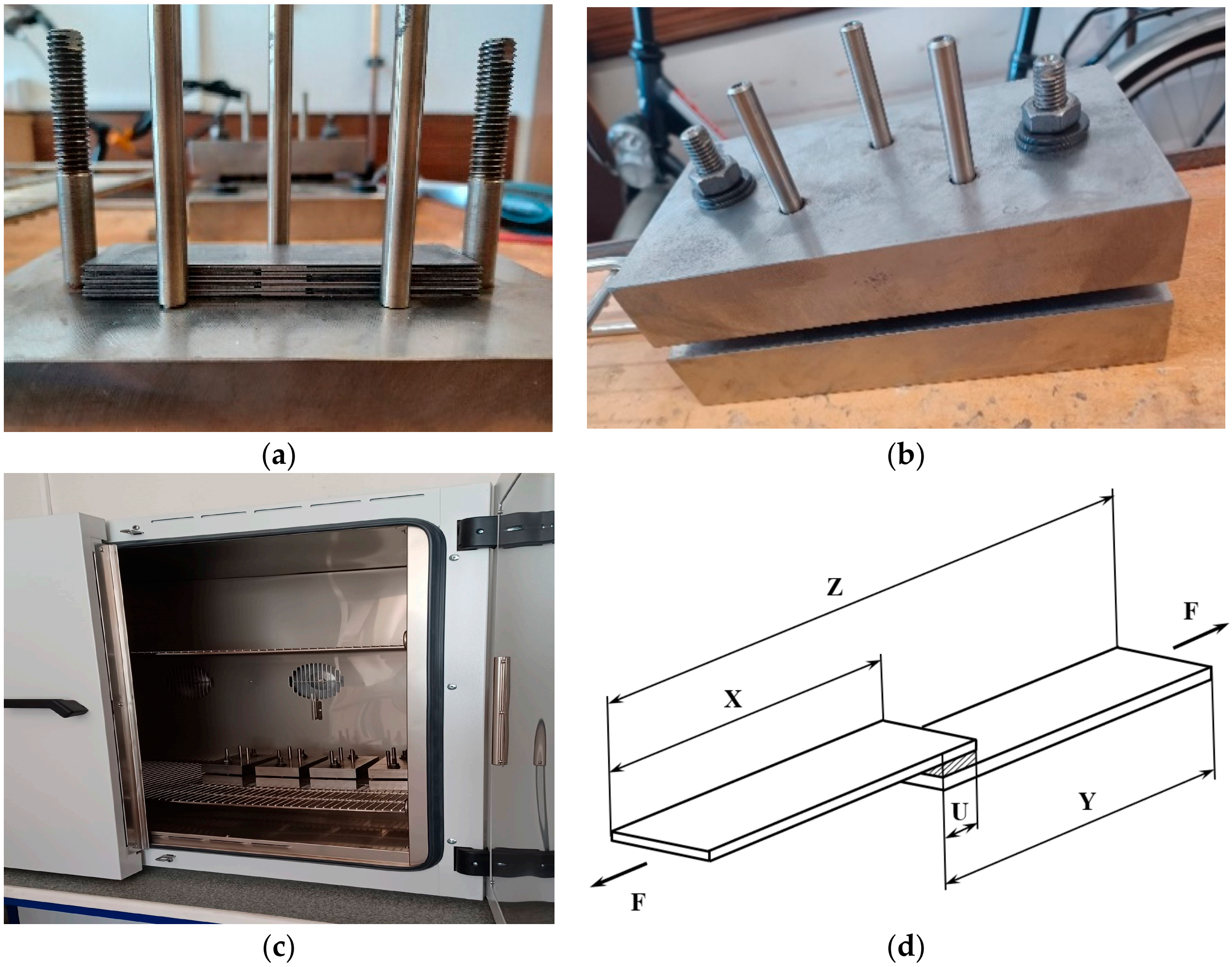

Figure 2. The sample preparation for the tensile lap-shear test: (**a**) the samples placed in the pressing tool; (**b**) the pressing tool; (**c**) the oven for the curing process of the insulating varnish; and (**d**) a scheme of the glued sample (Z, the total length of the glued samples; X, the sample length; No. 1, Y-sample length; and No. 2, U-length of glued joint).

The cut samples were then stacked in a pressing tool, with samples containing insulation (5 pairs) and samples without insulation (used to fill gaps in the pressing tool) placed alternately according to a specified arrangement (Figure 2a). The upper part of the tool was subsequently positioned and secured with screws to achieve a pressure of 3 MPa (Figure 2b). The assembly was then heated by placing the pressing tool with the samples in a preheated oven at 210 °C for 2 h (Figure 2c). After heating, the pressing tool and samples were allowed to cool naturally to an ambient temperature, a process that lasted approximately 4 h without air conditioning or a fan.

The test was conducted on a ZWICK Z010 testing machine (ZwickRoell GmbH&Co. KG, Ulm, Germany)—Figure 3. During testing, the maximum breakaway force (Fmax) was measured for each specimen. The lap-shear strength of the joint (τ_{max}) was then calculated based on the area of the glued lap joint. Subsequently, the average lap-shear strength and its standard deviation were determined for each steel grade.

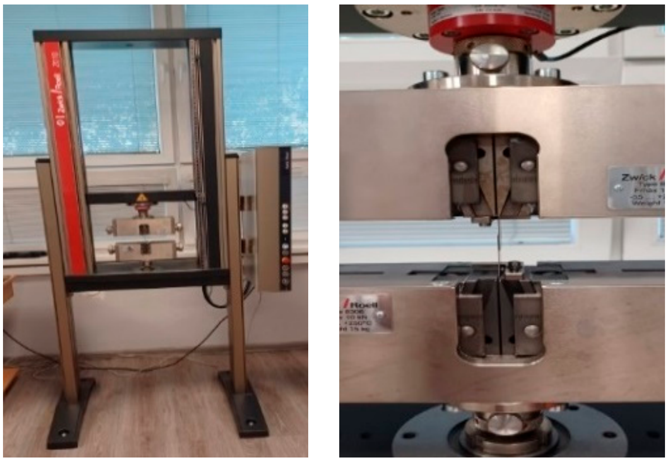

Figure 3. The tensile lap-shear test—testing machine ZWICK Z010.

2.3. Adhesion of Self-Bonding Varnish Layer

A bending test was conducted using the BYK 5710 device (BYK-Gardner GmbH, Geretsried, Germany) to evaluate the adhesion of the self-bonding varnish following the sample bending (Figure 4). The test assessed both the flexibility of the self-bonding varnish and its adhesion to the substrate to ensure that no disruption occurs during the subsequent processing. The specimens were bent to a 90° angle around a cylinder with a radius of 5 mm. After bending, the top and bottom surfaces at the bend radius were documented at 12.5× and 50× magnifications. The metallographic analysis of the interlayers was performed using a light microscope Olympus BXFM (Olympus, Tokyo, Japan) at a 500× magnification.

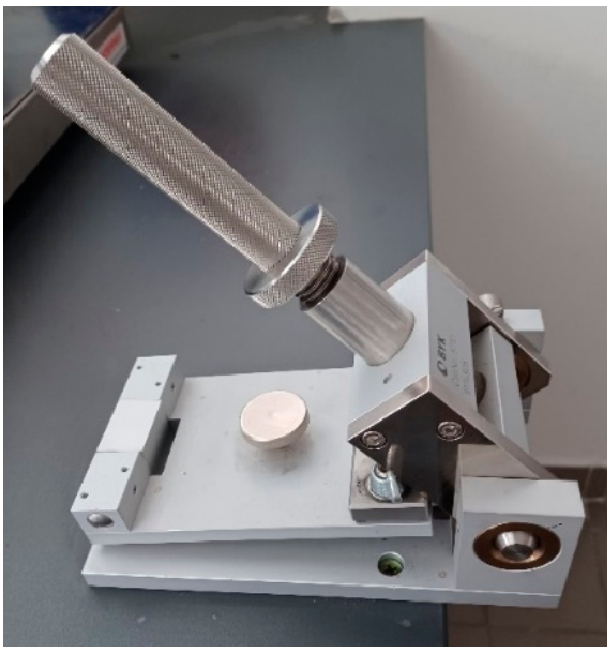

Figure 4. The BYK 5710 device for the bending test.

3. Results

3.1. Surface Microgeometry

The customers of non-oriented electrical steels require a minimum surface roughness of Ra = 0.6 µm. This surface finish was achieved during the cold rolling of the metal sheets using work rolls with a controlled surface roughness. For detailed surface characterization, not only was the surface roughness Ra measured, but additional roughness parameters, such as the Rz and the RPc, were also evaluated, which describe the microgeometry of the surface in greater detail. The calculated average values of the Ra, the Rz, and the RPc, which were measured perpendicular to the direction of the varnish application on the specimens produced under both dry and humid atmospheres and on both sides of each specimen, are shown in Table 5 and depicted in Figure 5. The results indicate that the required limit values were achieved under all production conditions. From a visual point of view, the surface quality of all samples was satisfactory, with no observable defects.

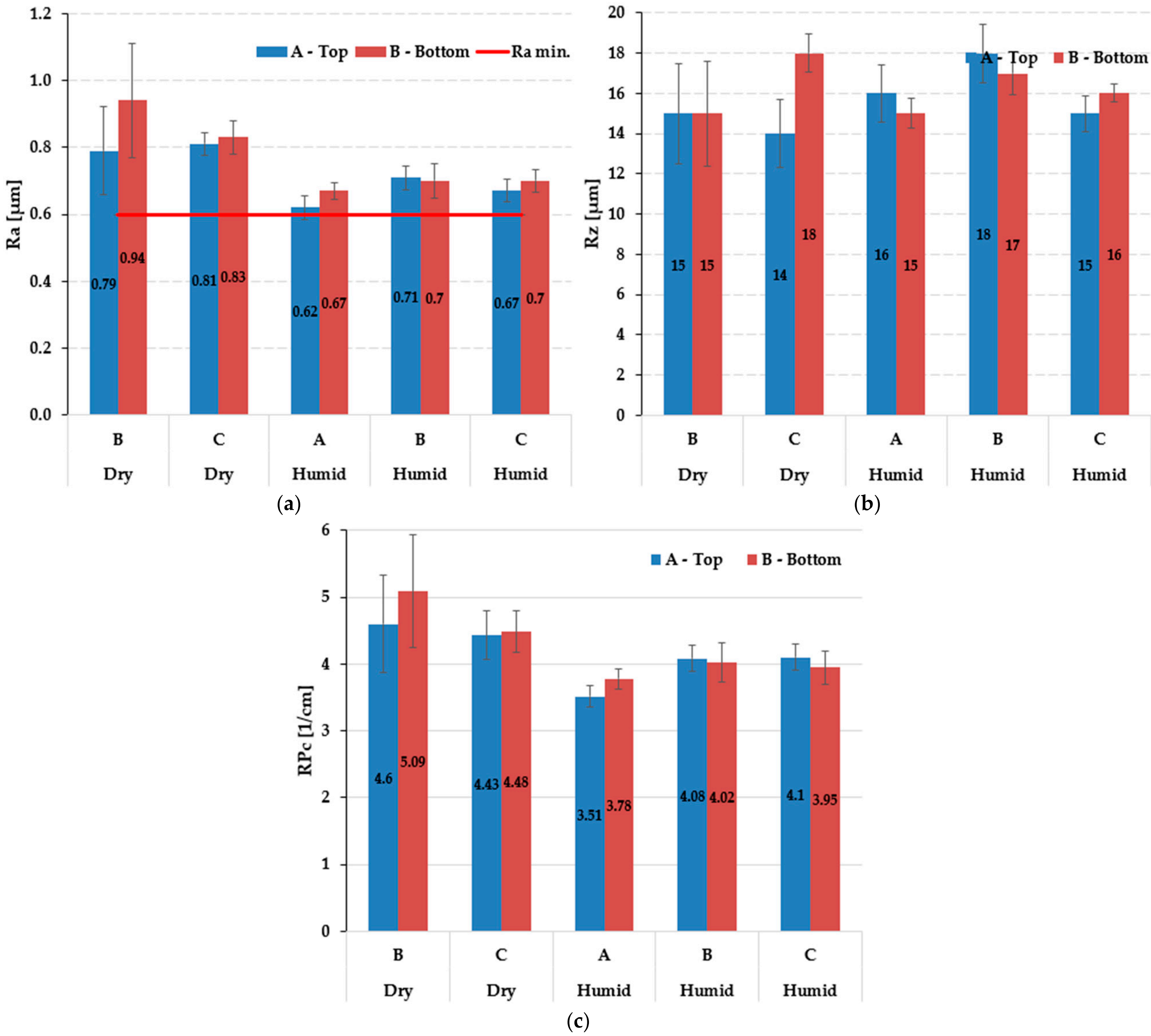

Figure 5. The average values of the surface roughness parameters: (**a**) Ra; (**b**) Rz; and (**c**) RPc.

Table 5. The average values of surface microgeometry parameters of the tested samples.

Steel Grade	Atmosphere	Top			Bottom		
		Ra [µm]	RPc [1/cm]	Rz [µm]	Ra [µm]	RPc [1/cm]	Rz [µm]
(B) STDEV	Dry	0.79 ±0.264	15 ±5.0	4.60 ±1.449	0.94 ±0.339	15 ±5.2	5.09 ±1.682
(C) STDEV	Dry	0.81 ±0.070	14 ±3.4	4.43 ±0.720	0.83 ±0.101	18 ±1.9	4.48 ±0.624
(A) STDEV	Humid	0.62 ±0.072	16 ±2.8	3.51 ±0.321	0.67 ±0.052	15 ±1.5	3.78 ±0.299
(B) STDEV	Humid	0.71 ±0.071	15 ±2.9	4.08 ±0.393	0.70 ±0.104	17 ±2.1	4.02 ±0.593
(C) STDEV	Humid	0.67 ±0.068	15 ±1.8	4.10 ±0.396	0.70 ±0.067	16 ±0.9	3.95 ±0.497

3.2. Tensile Lap-Shear Test

The results of the tensile lap-shear test for the specimens produced under both dry and humid atmospheres are presented in Tables 6 and 7, respectively. As shown, the thickness of the self-bonding varnish measured on both sides of each specimen determined the total bond thickness, which was controlled through the proper marking of the specimens during the lap joint preparation.

Table 6. The lap-shear strength and thickness of the self-bonding varnish for the samples produced in a dry atmosphere.

Steel Grade	Si and Al Content	Sample Designation Along Length Strip	Thickness of Self-Bonding Varnish Top	Bottom	Bond Thickness	Lap-Shear Strength τ_{max}
			[µm]	[µm]	[µm]	[MPa]
(B)	Medium	B1	1.6	3.8	5.4	15.30 ± 0.95
		B2	2.6	3.8	6.4	18.20 ± 1.40
		B3	3.0	3.0	6.0	16.30 ± 1.54
		B4	3.4	3.3	6.7	17.70 ± 0.55
(C)	High	C1	4.0	3.3	7.3	14.00 ± 2.51
		C2	3.5	3.2	6.7	20.00 ± 0.75
		C3	3.6	3.2	6.8	19.40 ± 0.75

For the (B) grade steel that was produced in a dry atmosphere, the highest lap-shear strength from the tensile test, τ_{max} = 18.20 ± 1.40 MPa, was achieved by sample B2, which corresponded to the highest RTF and the lowest HF and PMT recorded for the (B) grade. The thickness of the self-bonding varnish layer was 6.4 µm.

For steel grade (C), the highest lap-shear strength, τ_{max} = 20.0 ± 0.75 MPa, was observed in sample C2, which was produced at the lowest RTF, HF, and PMT for this grade. The corresponding self-bonding varnish layer thickness was 6.7 µm.

In regard to the non-oriented electrical steels produced in a humid atmosphere, the highest lap-shear strength from the tensile test, τ_{max} = 18.0 ± 0.67 MPa, was observed in sample A4, which corresponded to the highest RTF and the second lowest HF and PMT for the (A) grade. The thickness of the self-bonding varnish layer was 6.4 µm.

Table 7. The lap-shear strength and thickness of the self-bonding varnish for the samples produced in a humid atmosphere.

Steel Grade	Si and Al Content	Sample Designation Along Length Strip	Thickness of Self-Bonding Varnish Top [μm]	Bottom [μm]	Bond Thickness [μm]	Lap-Shear Strength τ_{max} [MPa]
(A)	Low	A1	2.9	2.9	5.8	16.30 ± 0.40
		A2	3.9	4.1	8.0	16.50 ± 0.85
		A3	2.2	2.5	4.7	16.20 ± 0.60
		A4	3.2	3.2	6.4	18.00 ± 0.67
		A5	3.1	2.9	6.0	17.70 ± 0.21
(B)	Medium	B1	2.9	2.9	5.8	16.47 ± 0.61
		B2	2.6	2.5	5.1	16.50 ± 1.18
		B3	3.1	2.8	5.9	14.40 ± 3.27
(C)	High	C1	2.6	2.5	5.1	3.70 ± 0.61
		C2	2.9	3.3	6.2	19.10 ± 0.62
		C3	2.9	2.8	5.7	18.90 ± 0.61

Steel grade (B) has shown the best lap-shear strength, τ_{max} = 16.5 ± 1.18 MPa, in sample B2, where the process parameters were as follows: RTF was the second-highest, HF was the lowest, and PMT was the second-lowest. The self-bonding varnish layer thickness was 5.1 μm.

Regarding steel grade (C), the highest lap-shear strength, τ_{max} = 19.10 ± 0.62 MPa, was obtained in sample C2, which was produced at the lowest RTF, second-highest HF, and lowest PMT for this grade. The corresponding self-bonding varnish layer thickness was 6.2 μm. Conversely, the lowest lap-shear strength, τ_{max} = 3.7 ± 0.61 MPa, was recorded for sample C1, which was produced under a humid atmosphere with the highest RTF, HF, and PMT.

The highest RTF, HF, and PMT values were recorded for steel grade (C) and were also the highest among all the evaluated samples, including steel grades (A) and (B). The highest temperatures of (A) and (B) were deliberately set beyond the production limits for steel grade (C) to examine the boundary conditions. The self-bonding varnish thickness was 5.1 μm. When the required minimum lap-shear strength, τ_{max} = 10 MPa, was not achieved, these samples and their corresponding production parameters were classified as non-compliant (NOK). Sample C1 (humid atmosphere) was the only sample among all of those tested that failed to reach the required τ_{max} value. Based on the lowest observed value of τ_{max} = 3.7 MPa, the RTF, HF, and PMT production parameters were adjusted, resulting in increased τ_{max} values for samples C2 and C3 (humid atmosphere), as shown in Table 7.

The lap-shear strength values, measured by the tensile lap-shear test for each steel grade, are depicted in Figure 6a (dry atmosphere) and Figure 6b (humid atmosphere) and are compared against the minimum limit value of 10 MPa.

The correlation between the measured lap-shear strength values and the selected processing parameters is presented in Figure 7. Within the investigated roughness range of 0.62–0.95 μm, no significant correlation between the surface roughness Ra and the lap-shear strength was observed. The joint strength remained relatively constant under both dry and humid conditions.

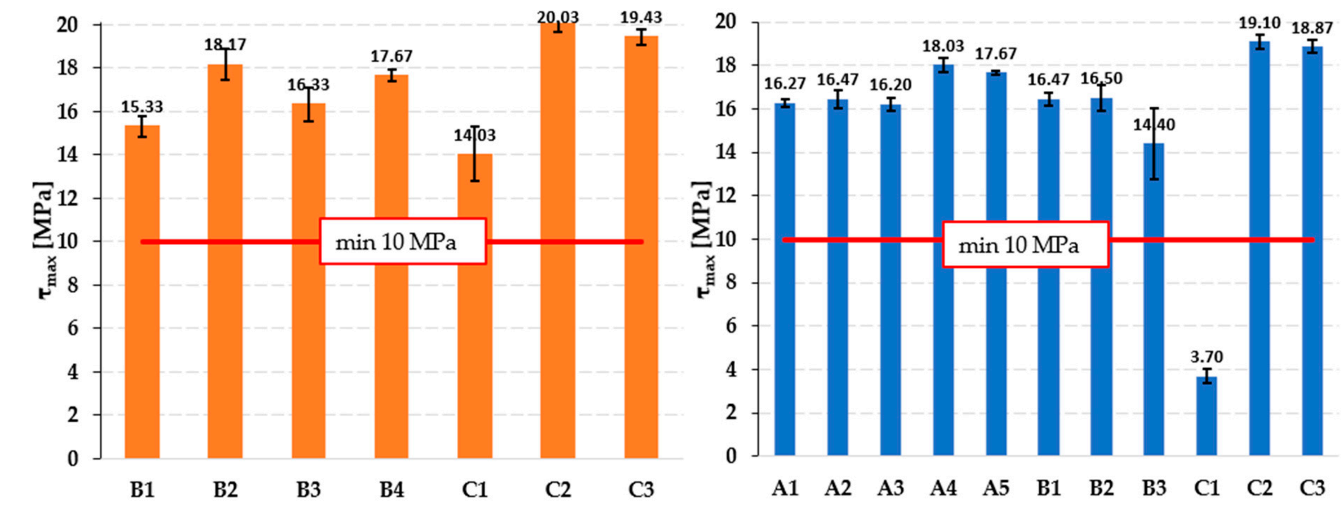

(**a**) (**b**)

Figure 6. The lap-shear strength measured for individual samples: (**a**) dry atmosphere and (**b**) humid atmosphere.

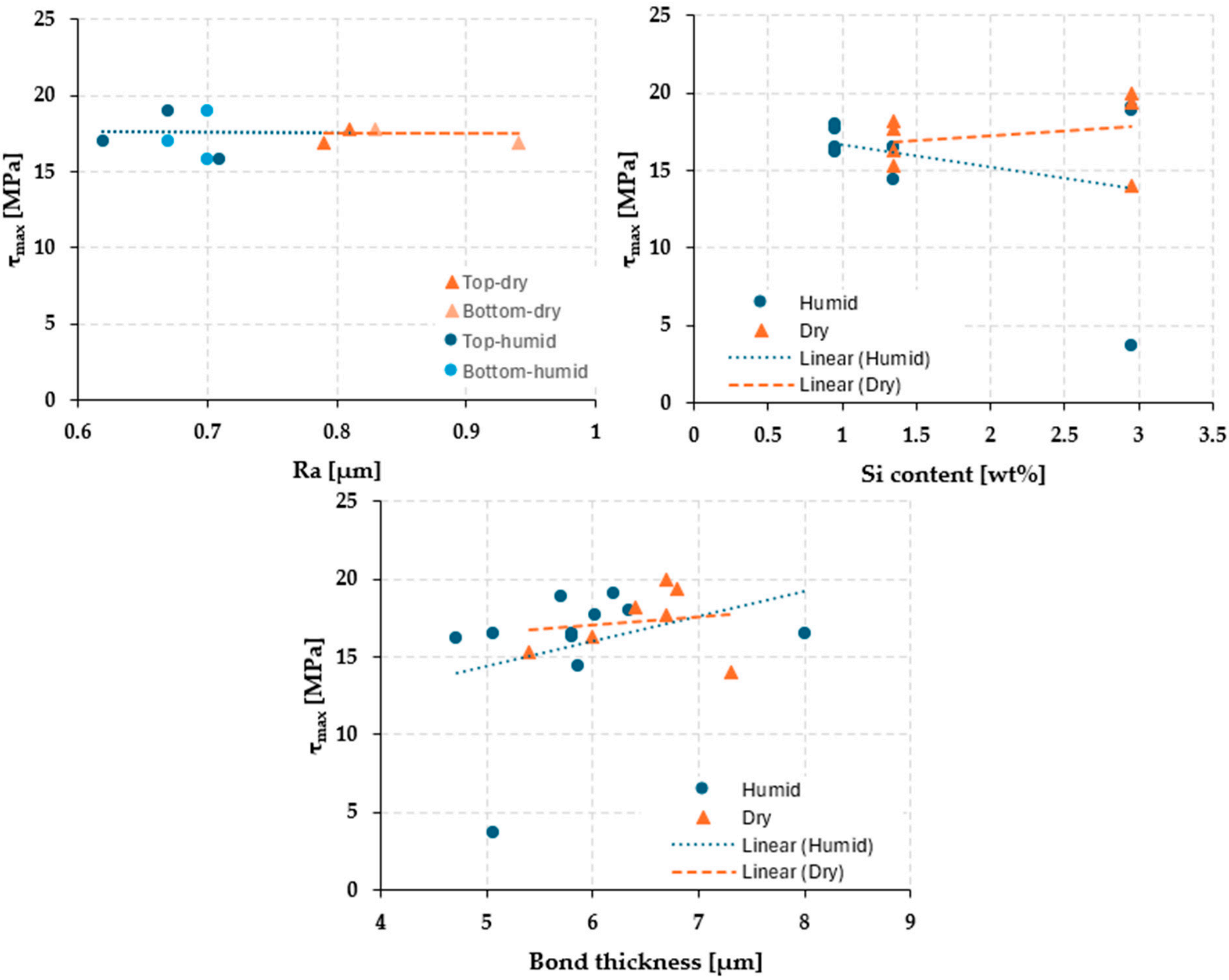

Figure 7. The influence of the selected parameters on the shear strength, τ_{max}.

When evaluating the influence of the Si content (0.95 to 2.95 wt.%) on the lap-shear strength, the results indicate that the effect is atmosphere-dependent. Under dry conditions, the strength remains relatively stable or slightly increases with the increasing Si content. In contrast, under humid conditions, a decreasing trend is observed, accompanied by an increased variability and a significant outlier at 2.95 wt.% Si. These findings suggest that a higher Si content may enhance the environmental sensitivity of the bonded interface.

A slight positive correlation between the bond thickness and the lap-shear strength was observed for both dry and humid conditions. The increasing bond thickness appears to enhance the joint performance, particularly under humid conditions, where thinner bonds exhibit greater variability and higher susceptibility to failure. These results indicate that maintaining an adequate bond thickness is important for ensuring reliable adhesion.

3.3. Adhesion of Self-Bonding Varnish Layer

The results of the bending test, performed to evaluate the adhesion of the self-bonding varnish layer to the substrate for the samples with the highest and lowest lap-shear strength values, are shown in Figure 8. The alternation of dark and light bands visible in Figure 8 is attributable to the method of varnish application using rollers. The bent regions of the samples (top/outside and bottom/inside) were examined visually after testing, revealing only a slight deterioration of the varnish layer in grade (C) with an Si content of 2.95% on both sides.

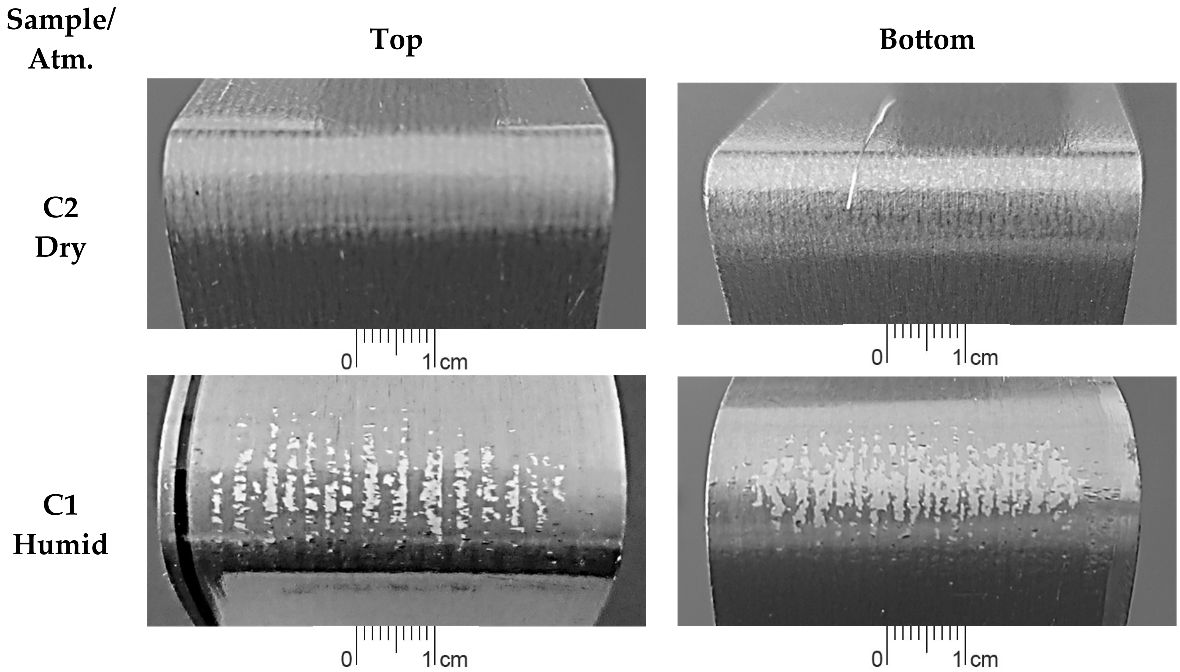

Figure 8. The macro images of the selected samples of electrical sheet metal with self-bonding varnish.

The bent regions were subsequently documented using an optical light microscope, Olympus GX 71 (Olympus, Tokyo, Japan), at 12.5× and 50× magnification, with a focus on evaluating the adhesion of the electro-insulating varnish on both the top and bottom sides of the sheet metal samples. A more detailed view of the samples with the highest and lowest lap-shear strength is shown in Figure 9. The varnish damage was observed, particularly in sample C1, which was annealed in a humid atmosphere. The mechanical damage or peeling occurs when the intermediate layer reaches a certain thickness, likely due to internal stresses within these layers. These stresses cause a mechanical degradation of the interlayers, which, in turn, affects the adhesion of the varnish to the steel substrate.

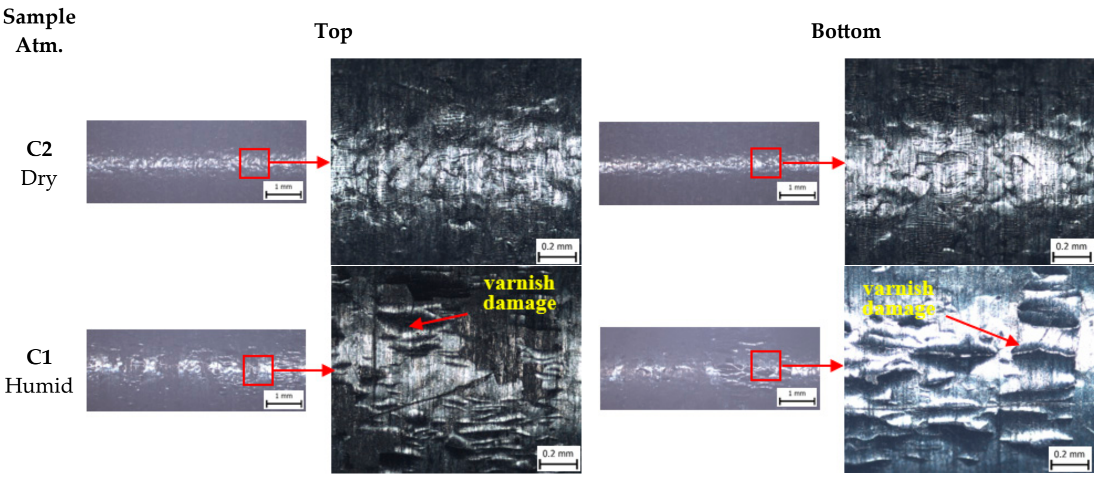

Figure 9. The details of the bent areas, optical microscope, 12.5× and 50× magnification.

The longitudinal metallographic sections were prepared and examined using a digital light microscope, Keyence VHX–5000 (Keyence, Osaka, Japan), at a magnification of 1000×. The selected regions of the metallographic sections, focusing on the intensity of the interlayer, are shown in Figure 10. For sample C2, which was annealed in a dry atmosphere, the interlayer thickness was 8.3 µm on the top side and 15.6 µm on the bottom side. A more pronounced interlayer was observed for sample C1, which was annealed in a humid atmosphere, with a thickness of 15.1 µm to 23.1 µm on the top side and 11.2 µm on the bottom side. In cases with intense and continuous interlayers, the adhesion of the electro-insulating varnish at the bend region was more severely compromised.

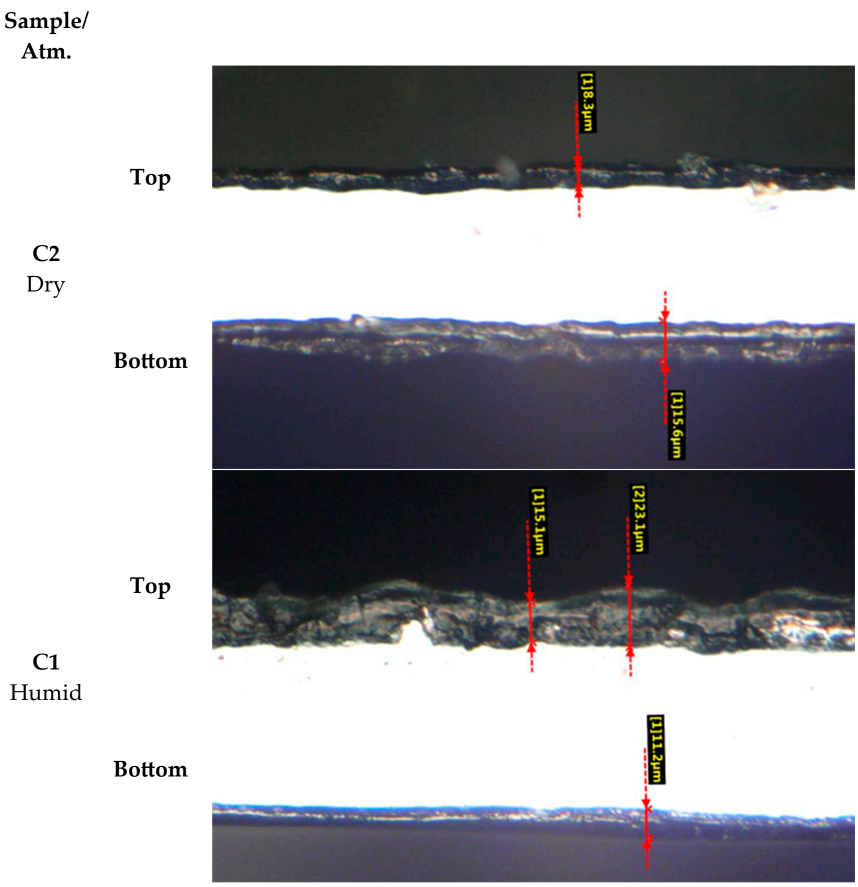

Figure 10. The selected parts of a metallographic section of a steel substrate—digital light microscope.

3.4. Influence of Production Parameters

The correlation between the measured lap-shear strength values and the production parameters is presented in Figure 11. The correlation between the RTF and the lap-shear strength indicates only a minor sensitivity to temperature fluctuation under both dry and humid annealing conditions. In a dry atmosphere, a slight decrease in strength is observed at higher temperatures, whereas under a humid atmosphere, a slight upward trend is evident. The major outlier, corresponding to a lap-shear strength of 3.7 MPa, is also highlighted.

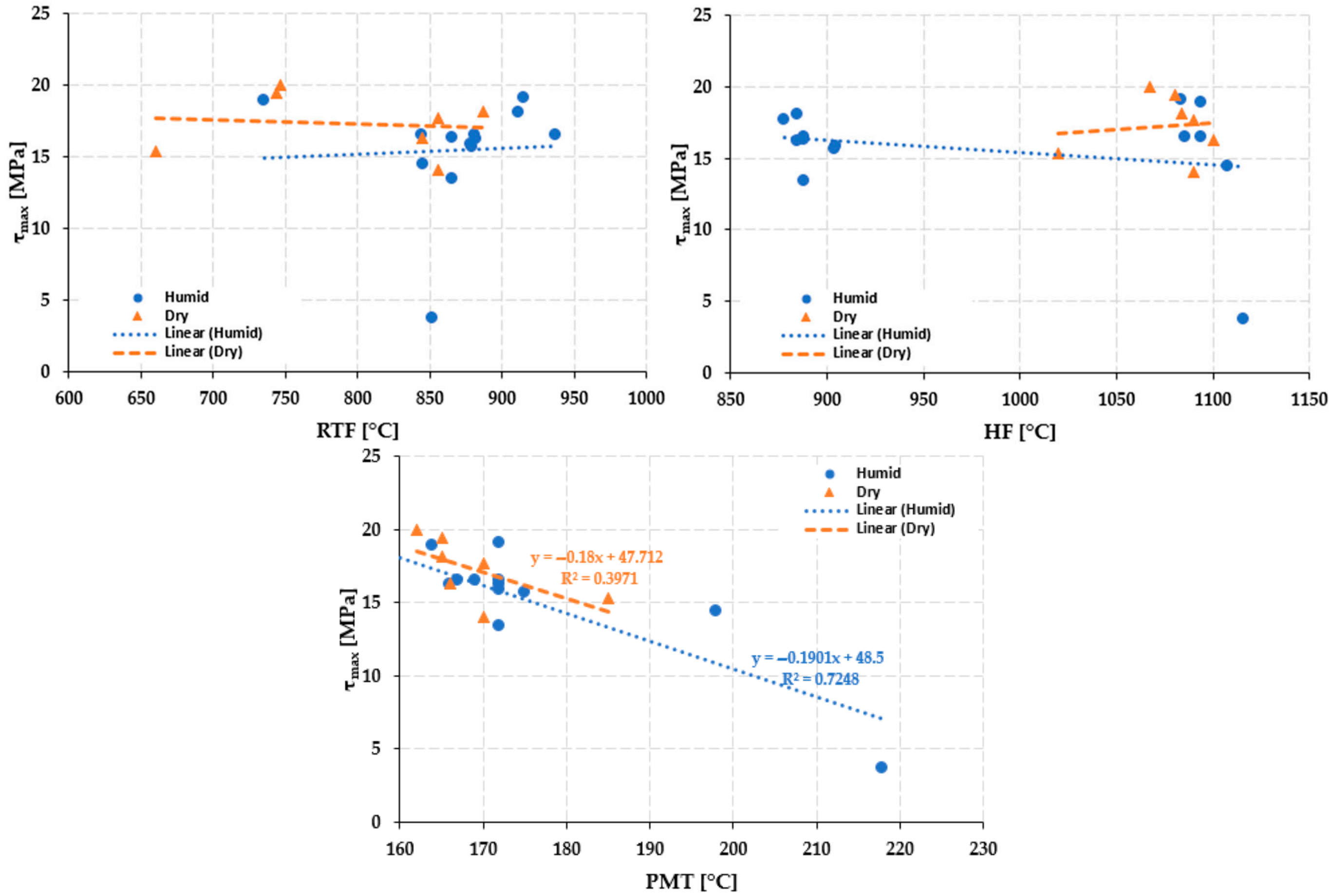

Figure 11. The influence of the PMT curing temperature on the lap-shear strength τ_{max}.

The correlation between the HF and the lap-shear strength indicates a progressive decline in shear strength under a humid annealing atmosphere, although the trend is influenced by the outlier at 3.7 MPa, which likely results from the combined effects of high temperature and humidity. Under annealing in a dry atmosphere, the lap-shear strength is largely retained, with a slight positive correlation observed across the temperature range.

The correlation between PMT and the lap-shear strength demonstrates a linear decrease in strength for both humid and dry annealing atmospheres as the PMT increases. The humid atmosphere exhibits higher sensitivity to thermal exposure, with a critical loss of integrity observed at 218 °C. The linear trend lines indicate that, although the rate of strength loss is similar across both environments, dry conditions consistently maintain a higher lap-shear strength across the tested thermal range.

Based on the presented trends, it can be concluded that the lap-shear strength is highly sensitive to the PMT, particularly under humid annealing conditions. The variations in the RTF and the HF result in marginal fluctuations in strength; however, exceeding a PMT over

200 °C in a humid atmosphere leads to a radical reduction in the lap-shear strength. The highest tensile lap-shear strength values for each steel grade were obtained at the lowest PMTs under both humid and dry annealing atmospheres.

4. Discussion

Flat-rolled non-oriented electrical steel is engineered to achieve target magnetic properties through precise control of microstructure. These properties are governed by crystallographic features such as grain size, texture, and defects. Silicon, as the primary alloying element, increases the electrical resistivity, reduces eddy current losses, and stabilizes the crystal structure, while also influencing grain growth kinetics and the development of preferred orientations. Aluminum and manganese primarily serve metallurgical functions—such as refining grain structure, thereby reducing the hysteresis component of core losses—rather than directly affecting physical properties like volume resistivity [19,26]. Li et al. [27] reported that the addition of an Fe–RE–Si alloy effectively modifies the chemistry and morphology of inclusions in silicon steel, resulting in stable RE_2O_2S-based inclusions and a coarsening of the inclusion size, which may have significant implications for the magnetic properties of the steel.

The applied continuous annealing conditions governed the microstructure evolution through recovery, recrystallization, and grain growth, all of which are critical for the resulting magnetic properties. The decarburization, conducted in a humid atmosphere, effectively reduced the carbon content and suppressed the carbide formation, thereby facilitating the development of a defect-reduced crystal lattice. This is essential for preventing the aging effects that are associated with carbon-induced lattice distortions. When the initial carbon level was sufficiently low, processing in a dry atmosphere (dew point < -15 °C) proved adequate, indicating that carbon control primarily influences the defect density rather than the recrystallization kinetics [23,24].

The elevated temperatures in the second furnace section promoted grain growth and texture evolution, resulting in an optimized crystallographic structure. The low dew point (<-55 °C) further minimized impurity interactions, thereby supporting homogeneous grain development. These results confirm that controlled annealing conditions directly determine grain size, boundary characteristics, and crystallographic orientation, all of which are key factors governing the magnetic performance [28].

For the study of self-bonding varnish adhesion, the boundary conditions specified in Section 2.1.1 were verified. These processing windows allowed for the achievement of an optimal microstructure and a balanced combination of electrical and magnetic properties in accordance with the company standards.

Within the study, the initial surface roughness Ra of the experimental non-oriented electrical steels ranged from 0.62 to 0.95 μm. However, no significant correlation between the surface roughness Ra and the lap-shear strength was observed for either humid or dry annealing atmospheres. Boutar et al. [29] reported that the highest lap-shear strength was measured for a surface roughness of 0.6 μm, with only a slight decrease within the range of 0.6 to 1.5 μm. Similarly, Rudawska et al. [30] highlighted the importance of surface roughness on lap-shear strength.

The self-bonding varnish thickness used in this study (≈3 μm per side) lies at the lower limit of the recommended range [31]. A slight positive correlation between the bond thickness and the lap-shear strength was observed under both dry and humid conditions, which contrasts with previous findings. Chen et al. [32] showed that increasing the adhesive thickness and the lap length generally reduces the shear strength. Da Silva et al. [33] reported that the lap-shear strength decreases with increasing thickness for ductile and intermediate adhesives, whereas the brittle systems may exhibit non-monotonic behavior.

https://doi.org/10.3390/cryst16040253

Marchfelder et al. [34] reported that the new water-borne epoxy varnishes with thicknesses below 10 µm can benefit from silane-based adhesion promoters, which enhance the adhesion to steel substrates.

The study also revealed that among the processing parameters RTF, HF, and PMT, the lap-shear strength is highly sensitive to the PMT. An improved lap-shear strength was observed in both of the atmospheres at lower PMT values, following the same trend. Although a lower PMT may result in slightly under-cured joints with insufficient crosslink density, the overall joint strength was not significantly affected [13,35]. In contrast, the highest PMT (over 200 °C) combined with a humid atmosphere caused a rapid decrease in the lap-shear strength. Banea et al. [36] reported that a drastic drop in the lap-shear strength occurs if the glass transition temperature threshold is exceeded due to thermal degradation.

When evaluating the influence of the Si content (ranging from 0.95 to 2.95 wt.%) on the lap-shear strength, the results indicate that the strength is sensitive to the annealing atmosphere. A significant outlier was observed at 2.95 wt.% Si when processed in a humid atmosphere under specific processing conditions. The light microscopy revealed the presence of an interlayer on the steel substrate, indicating the formation of an oxide layer, as reported by several authors. Xie et al. [37] reported that the presence of surface oxide scales consistently led to a deterioration in the mechanical properties of the bonded joints. Diéz-Ercilla et al. [38] demonstrated that the growth of this layer depends on both the temperature of the treatment and the silicon content in the steel. Song et al. [39] concluded that high-silicon steels exhibit a significantly lower oxidation rate compared to low-silicon steels under the same high-temperature conditions.

Under various technological processing conditions for steels (A), (B), and (C) at RTF, HF, and PMT, the influence of both the chemical concept and technological parameters on the lap-shear strength and the varnish adhesion was demonstrated. The presence and extent of the layer on the evaluated non-oriented electrical steels will be the subject of further research, in which EDX/SEM analyses will be employed to confirm the presence of oxides and determine their composition.

5. Conclusions

This study evaluated the impact of selected initial material and surface properties—steel surface roughness, varnish (bond) thickness, and Si content—as well as the process-relevant parameters, including annealing atmosphere, decarburization temperature (RTF), heating furnace or grain growth temperature (HF), and varnish curing temperature (PMT), on the adhesion of self-bonding varnish as assessed by the lap-shear test. The following conclusions are drawn:

- The lap-shear strength of the self-bonded non-oriented electrical steels was found to be independent of the surface roughness within the investigated range, indicating that the applied surface preparation was sufficient to ensure consistent adhesion.
- The Si content exhibited condition-dependent effects. A higher Si content enhances the sensitivity of the bonded interface to the environmental factors, decreasing the strength and increasing the variability under a humid atmosphere. This may reflect changes in the surface oxide characteristics.
- The bond thickness showed a weak positive influence on the strength, particularly in the moisture-exposed environments.
- While the RTF and the HF resulted in relatively stable mechanical performance between 650 °C and 1100 °C, the PMT was identified as the critical factor. The strong negative correlation confirms that the PMT is the primary determinant of the lap-shear strength degradation.

https://doi.org/10.3390/cryst16040253

- Humidity plays an important role in mechanical performance. Across the thermal ranges, samples that were annealed under a humid atmosphere exhibited lower lap-shear strength than those processed in a dry atmosphere, which suggests that moisture likely facilitates the interfacial oxidation of the bonding matrix.
- The drastic reduction in the lap-shear strength to 3.7 MPa does not appear to be a random error but rather a predictable threshold event. This outlier occurs when the material is subjected to the synergic effect of a high PMT and a humid atmosphere.
- To maintain a lap-shear strength above 15 MPa, processing should be controlled to keep the PMT below 180 °C. If higher temperatures are required for processing, dry annealing conditions must be employed.

The proper selection of process-relevant parameters for the production of non-oriented electrical steels, with regard to the adhesion of the self-bonding varnish, ensures the sufficient quality of the laminations in the stator. Thus, for individual grades (A), (B), and (C), the lowest RTF, HF, and PMT should be used. The stators prepared under these conditions offer several advantages, including improved mechanical stability, enhanced electrical performance, reduced eddy current losses, minimized vibrations and noise, and better magnetic properties with lower core losses.

Author Contributions: Conceptualization, S.N. and V.T.; methodology, V.T. and M.H.; validation, M.H. and V.K.; formal analysis, J.S.; investigation, M.H., V.K., V.T., A.G. and I.F.; resources, S.N.; data curation, S.N. and V.K.; writing—original draft preparation, M.T. and S.N.; writing—review and editing, M.T. and S.N.; visualization, V.T.; supervision, E.E.; funding acquisition, M.T., E.E. and J.S. All authors have read and agreed to the published version of the manuscript.

Funding: This study was funded by the Scientific Grant Agency of the Ministry of Education, Research, Development and Youth of the Slovak Republic and the Slovak Academy of Sciences (VEGA) and the Slovak Research and Development Agency (APVV).

Data Availability Statement: The data are only available on request due to restrictions provided by the funder.

Acknowledgments: This study was accomplished under the grant projects VEGA 1/0238/23, VEGA 1/0609/25, and VEGA 1/0539/23, as well as the research project APVV SK-PL-25-0118.

Conflicts of Interest: Authors Vanda Tomková, Stanislav Németh, Vladimír Kundracik, and Iveta Filipovská are employed by the company U.S. Steel Košice s.r.o. The author Matúš Horváth is employed by the company Magna Powertrain, s.r.o. The remaining authors declare that the research was conducted in the absence of any commercial or financial relationships that could be construed as potential conflicts of interest.

References

1. Schneider, M.; Urban, N.; Franke, J. Relation of joining parameters of stator core production and iron loss. In Proceedings of the 2017 7th International Electric Drives Production Conference (EDPC), Würzburg, Germany, 5–6 December 2017; pp. 1–6. [CrossRef]
2. Schonherr, R. TGA-FTIR-Kopplung Anwendung zur Untersuchung von ElektroIsolier-Lacken (Backlack). *Mater. Werkst.* **1996**, *27*, 267–271. [CrossRef]
3. In-Depth Study of Self-bonding Motor Lamination Stacks. Available online: https://www.backlack.com/News/in-depth-study-of-self-bonding-motor-lamination-stacks.html (accessed on 6 September 2025).
4. Poskovic, E.; Ferraris, L.; Bramerdorfer, G.; Cossale, M. A Thermographic Method to Evaluate Different Processes and Assembly Effects on Magnetic Steels. *IEEE Trans. Ind. Appl.* **2022**, *58*, 3405–3413. [CrossRef]
5. Bali, M.; Muetze, A. The degradation depth of non-grain oriented electrical steel sheets of electric machines due to mechanical and laser cutting: A state-of-the-art review. *IEEE Trans. Ind. Appl.* **2019**, *55*, 366–375. [CrossRef]
6. Coatings for Electric Vehicles. Available online: https://www.kansai-helios.at/en/markets-products/core-plate-varnishes/e-mobility/ (accessed on 6 September 2025).

7. Motor Bonding Lamination Stacks. Available online: https://lammotor.com/glue-bonding-stator-rotor/ (accessed on 6 September 2025).
8. Electrical Steel Strip with Precise Magnetic Properties. Available online: https://www.waelzholz.com/en/steel-materials/electrical-steel-strip.html (accessed on 6 September 2025).
9. Mahmouditabar, F.; Baker, N. A Review on the Effect of Electrical Steel Manufacturing Processes on the Performance of Electric Machines. *Energies* **2023**, *16*, 7954. [CrossRef]
10. Xia, C.; Wang, H.; Wu, Y.; Wang, H. Joining of the Laminated Electrical Steels in Motor Manufacturing: A Review. *Materials* **2020**, *13*, 4583. [CrossRef]
11. Insulating Varnish Systems. Available online: https://www.voestalpine.com/isovac/en/Products/Insulating-varnish-systems (accessed on 6 September 2025).
12. Baloglu, M.V.; Ziegler, M.; Franke, J.; Willner, K. Determination of Equivalent Transversely Isotropic Material Parameters for Sheet-Layered Lamination Stacks. *Mech. Syst. Signal Process.* **2020**, *145*, 106915. [CrossRef]
13. Marchfelder, C.; Pugstaller, R.; Wallner, G.M.; Brüggemann, O.; Aufray, M. Effect of Epoxy Structure on Properties of Waterborne Coatings and Electrical Steel Laminates. *Polymers* **2022**, *14*, 1556. [CrossRef]
14. Backlack: Testing Methods and Production of Test Specimens. Available online: https://www.voestalpine.com/isovac/en/insights/self-bonding-varnish-testing-methods-and-production-of-test-specimens (accessed on 7 September 2025).
15. *EN 1464:2010*; Adhesives—Determination of Peel Resistance of Adhesive Bonds—Floating Roller method. European Committee for Standardization (CEN): Brussels, Belgium, 2010.
16. *EN 1465:2009*; Adhesives—Determination of Tensile Lap-Shear Strength of Bonded Assemblies. European Committee for Standardization (CEN): Brussels, Belgium, 2009.
17. Garrison, W.M. Steels: Classifications. In *Encyclopedia of Materials: Science and Technology*; Buschow, K.H.J., Cahn, R.W., Flemings, M.C., Ilschner, B., Kramer, E.J., Mahajan, S., Veyssière, P., Eds.; Elsevier: Oxford, UK, 2001; pp. 8840–8843.
18. Ouyang, G.; Chen, X.; Liang, Y.; Macziewski, C.; Cui, J. Review of Fe-6.5 wt%Si High Silicon Steel—A Promising Soft Magnetic Material for Sub-kHz Application. *J. Magn. Magn. Mater.* **2019**, *481*, 234–250. [CrossRef]
19. Elgamli, E.; Anayi, F. Advancements in Electrical Steels: A Comprehensive Review of Microstructure, Loss Analysis, Magnetic Properties, Alloying Elements, and the Influence of Coatings. *Appl. Sci.* **2023**, *13*, 10283. [CrossRef]
20. Kim, M.S.; Chae, W.K.; Choe, H.J. Non-Oriented Electrical Steel Sheet and Manufacturing Method Therefor. EP 3 239 326 B1, 1 November 2024.
21. Leunis, E.; Van De Putte, T.; Jacobs, S.; Saikaly, W. Method of Production of Tin-Containing Non Grain-Oriented Silicon Steel Sheet, Steel Sheet Obtained and Use Thereof. EP3 209 807 A1, 30 August 2023.
22. Yasiki, H.; Natori, Y.; Takeda, K.; Mukawa, S.; Matsumoto, T.; Fujita, K.; Morohoshi, T.; Miyazaki, M. Non-Oriented Electromagnetic Steel Sheet Having Excellent Magnetic Characteristics. EP3 569 728 A1, 20 November 2023.
23. Hilinski, E.J.; Johnston, G.H. Annealing of electrical steel. In Proceedings of the 2014 4th International Electric Drives Production Conference (EDPC), Nuremberg, Germany, 18–20 June 2014; pp. 1–7. [CrossRef]
24. Jin, X.; Chu, S.; Peng, J.; Hu, G. Effect of dew point on selective oxidation and decarburization of 0.2%C-1.5%Si-2.5%Mn high strength steel sheet during continuous annealing. *Acta Metall. Sin.* **2023**, *59*, 1324–1334. [CrossRef]
25. *ISO 21 920-2:2021*; Geometrical Product Specifications (GPS)—Surface Texture: Profile—Part 2: Terms, Definitions and Surface Texture Parameters. ISO: Geneva, Switzerland, 2021.
26. AK Steel Corporation. *Selection of Electrical Steels for Magnetic Cores*; Product Data Bulletin; AK Steel Corporation: West Chester, OH, USA, 2007.
27. Li, X.; Chen, C.; Wang, T.; Guo, Z.; Wang, H.; Wang, H.; Xue, L.; Tian, J.; Sun, Y. Inclusions and phases in Fe-RE-Si steelmaking alloys and their effect on evolution of inclusions in non-oriented silicon steels. *J. Rare Earths* **2026**, *44*, 377–387. [CrossRef]
28. Wang, L.; Wang, S.; Li, J.; Zhang, M.; Feng, Y. Effects of High-Temperature Annealing Atmosphere on the Secondary Recrystallization Behavior and Magnetic Properties of Fe-3.2%Si-0.055%Nb Grain-Oriented Silicon Steel. *Materials* **2022**, *15*, 8388. [CrossRef]
29. Boutar, Y.; Naïmi, S.; Mezlini, S.; Ali, M.B.S. Effect of Surface Treatment on the Shear Strength of Aluminium Adhesive Single-Lap Joints for Automotive Applications. *Int. J. Adhes. Adhes.* **2016**, *67*, 38–43. [CrossRef]
30. Rudawska, A.; Miturska-Barańska, I.; Doluk, E. Influence of Surface Treatment on Steel Adhesive Joints Strength—Varnish Coats. *Materials* **2021**, *14*, 6938. [CrossRef]
31. Kim, J.; Ha, B.; Lee, D.; Park, J. Self-Bonding Electrical Steel Sheet and Laminate Comprising the Same. Korean Patent KR20220089675A, 28 June 2022.
32. Chen, Q.; Du, B.; Zhang, X.; Zhong, H.; Ning, C.; Bai, H.; Li, Q.; Pan, R.; Zhou, B.; Hu, H. Parametric Investigation into the Shear Strength of Adhesively Bonded Single-Lap Joints. *Materials* **2022**, *15*, 8013. [CrossRef]
33. Da Silva, L.F.M.; Rodrigues, T.N.S.; Figueiredo, M.V.; de Moura, M.F.S.F.; Öchsner, A. Effect of adhesive type and thickness on the lap shear strength. *J. Adhes.* **2006**, *82*, 1053–1076. [CrossRef]

34. Marchfelder, C.; Pugstaller, R.; Wallner, G.M. Effect of Adhesion Promoters on Rheokinetics and Roll Peel Strength of Electrical Steel Stacks. *Int. J. Adhes. Adhes.* **2024**, *134*, 103789. [CrossRef]
35. Tiefenthaler, M.; Wallner, G.M.; Marchfelder, C.; Strauß, B. Simulation of steel/epoxy laminates for electric engines or generators: Part 2—Experimentally and numerically established temperature-dependent cohesive zone model. *J. Mater. Sci.* **2025**, *60*, 9969–9984. [CrossRef]
36. Banea, M.D.; da Silva, L.F.M.; Campilho, R.D.S.G. Effect of Temperature on the Shear Strength of Aluminium Single Lap Bonded Joints for High Temperature Applications. *J. Adhes. Sci. Technol.* **2014**, *28*, 1367–1381. [CrossRef]
37. Xie, B.; Sun, M.; Xu, B.; Wang, C.; Li, D.; Li, Y. Dissolution and evolution of interfacial oxides improving the mechanical properties of solid state bonding joints. *Mat. Des.* **2018**, *157*, 437–446. [CrossRef]
38. Diéz-Ercilla, M.; Ros-Yáñez, T.; Petrov, R.; Houbaert, Y.; Colás, R. Oxidation of Silicon Steels. *Corros. Eng. Sci. Technol.* **2004**, *39*, 295–300. [CrossRef]
39. Song, E.J.; Suh, D.W.; Bhadeshia, H.K.D.H. Oxidation of Silicon Containing Steel. *Ironmak. Steelmak.* **2012**, *39*, 599–604. [CrossRef]